Published in final edited form as:
Vascul Pharmacol. 2012 ; 56(1-2): 64–73. doi:10.1016/j.vph.2011.11.002.

Resveratrol Reverses Monocrotaline-Induced Pulmonary Vascular and Cardiac Dysfunction: A Potential Role for Atrogin-1 in Smooth Muscle

Michael L. Paffett, **Selita N. Lucas**, and **Matthew J. Campen**
College of Pharmacy, Division of Pharmaceutical Sciences, University of New Mexico Health Sciences Center, Albuquerque, NM 87131-0001

Abstract

Arterial remodeling contributes to the elevated pulmonary artery (PA) pressures and right ventricular hypertrophy seen in pulmonary hypertension (PH). Resveratrol, a sirtuin-1 (SIRT1) pathway activator, can prevent the development of PH in a commonly used animal model, but it is unclear whether it can reverse established PH pathophysiology. Furthermore, atrophic ubiquitin ligases, such as atrogin-1 and MuRF-1, are known to be induced by SIRT1 activators but have not been characterized in hypertrophic vascular disease. Therefore, we hypothesized that monocrotaline (MCT)-induced PH would attenuate atrophy pathways in the PA while, conversely, SIRT1 activation (resveratrol) would reverse indices of PH and restore atrophic gene expression. Thus, we injected Sprague-Dawley rats with MCT (50 mg/kg i.p.) or saline at Day 0, and then treated with oral resveratrol or sildenafil from days 28–42 post-MCT injection. Oral resveratrol attenuated established MCT-induced PH indices, including right ventricular systolic pressure, right ventricular hypertrophy, and medial thickening of intrapulmonary arteries. Resveratrol also normalized PA atrogin-1 mRNA expression, which was significantly reduced by MCT. In cultured human PA smooth muscle cells (hPASMC), resveratrol significantly inhibited PDGF-stimulated proliferation and cellular hypertrophy, which was also associated with improvements in atrogin-1 levels. In addition, SIRT1 inhibition augmented hPASMC proliferation, as assessed by DNA mass, and suppressed atrogin mRNA expression. These findings demonstrate an inverse relationship between indices of PH and PA atrogin expression that is SIRT1 dependent and may reflect a novel role for SIRT1 in PASMCs opposing cellular hypertrophy and proliferation.

Keywords

phytoalexin; atrogin-1; smooth muscle hypertrophy; atrophy; ubiquitin-proteasome system; resveratrol

1. INTRODUCTION

Abnormal hypertrophy and hyperplasia of smooth muscle cells can lead to anatomical narrowing of lumens, both in the vasculature and airways. Numerous pathologies manifest

Address Correspondence to: Matthew J. Campen, PhD, MSPH College of Pharmacy MSC09 5360 1 University of New Mexico Albuquerque, NM 87131 Phone: (505) 925-7778 Fax: (505) 272-6749 mcampen@salud.unm.edu.

smooth muscle cell hypertrophy and proliferation, including idiopathic and secondary forms of pulmonary arterial hypertension (PH), atherosclerosis, and even in reactive airway diseases such as chronic asthma (Newby and Zaltsman, 2000; Siddiqui and Martin, 2008). Luminal narrowing results in increased resistance and, in the instance of PAH, an increase in right ventricular afterload and eventual maladaptive hypertrophy and ultimately right heart failure ensues (Humbert et al., 2004). There is general consensus that arterial remodeling is among the principal causes of increased resistance that, along with adventitial fibroblasts and endothelial cells transitioning to a mesenchymal phenotype (Stenmark et al., 2002) and increased endothelial proliferation (Budhiraja et al., 2004), contribute to a flow-restricted state in the diseased lung. While much is known regarding PASMC hypertrophic and proliferative pathways in PAH syndromes, the recently characterized molecular atrophy pathways, largely driven by the ubiquitin-proteasome system, have yet to be characterized in syndromes of abnormal vascular growth.

Atrophy-mediating E3 ubiquitin ligases, atrogin-1 and MuRF-1, play a significant role in regulating cardiac and skeletal muscle growth by selective proteasomal degradation of key proteins such as calcineurin (CnA), MyoD, and eIF3 (Lagirand-Cantaloube et al., 2009; Li et al., 2004; Csibi et al., 2009). Expression and activity of these E3 ubiquitin ligases oppose cellular hypertrophy and enhanced during calorie restriction and muscle wasting disorders (Hepple et al., 2008; McFarlane et al., 2006). Upstream regulators of atrogin-1 expression, such as F-box (Fox)-O transcription factors, induce atrophy and apoptosis in a number of muscle types (McLoughlin et al., 2009), but their role in smooth muscle atrophy is undocumented.

Interestingly, the polyphenolic compound, resveratrol, enhances transcriptional activity of FOXO1 through a sirtuin-1 dependent deacetylation mechanism in cardiomyocytes (Ni et al., 2006) and inhibits vascular smooth muscle proliferation (Poussier et al., 2005). Furthermore, atrogin-1 has been shown to attenuate pathological hypertrophy in cardiomyocytes driven by agonist-induced calcineurin (CnA)-dependent activation of NFATc4, whereas silencing of atrogin-1 with siRNA enhanced CnA/NFAT signaling and hypertrophy in cardiomyocytes (Li et al., 2004). Currently, there is a lack of information regarding the role of atrogin-1 or other E3 ubiquitin ligases in pathological vascular smooth muscle hypertrophy.

Resveratrol has recently been shown to prevent monocrotaline (MCT)-induced pulmonary hypertension, in part, by having anti-proliferative, anti-inflammatory and anti-oxidant effects in pulmonary vascular smooth muscle cells (Csiszar et al., 2009). Endothelial function was also improved in small intrapulmonary arteries where endothelial nitric oxide synthase (eNOS) expression was similarly enhanced by chronic resveratrol treatment. Although this study examined the preventative effects of resveratrol on MCT-induced vascular hypertrophy, information regarding the effect of resveratrol *reversing* established PAH is lacking (Chicoine et al., 2009). Furthermore, no information exists regarding pulmonary artery (PA) transcriptional regulation of the ubiquitin ligases, atrogin-1 and MuRF-1, during the development and persistence of experimentally induced pulmonary hypertension. Therefore, we investigated 1) whether chronic resveratrol administration could reverse established MCT-induced increases in right ventricular pressure and remodeling; 2) the temporal expression of ubiquitin ligases in pulmonary arteries from MCT-pulmonary hypertensive rats; 3) the effect of resveratrol on arterial atrogin-1 expression, right ventricular hypertrophy, and vascular function in the MCT model; and 4) the effect of resveratrol to stimulate atrogin expression

2. MATERIALS AND METHODS

All animal protocols were reviewed and approved by the Institutional Animal Care and Use Committee of Lovelace Respiratory Research Institute and the University of New Mexico. Rats were obtained from a commercial vendor (Charles River Laboratories) and were allowed to acclimate for 2 wks prior to experimentation, with food and water available *ad libitum*.

2.1 Experimental Design

In order to study a relatively stable and established remodeled vasculature with minimal contribution from inflammatory pathways, which peak around 14–21 days post-injection (Wilson et al., 1989), rats were treated with MCT 28 days prior to initiation of therapeutics. Pulmonary hypertension was generated in adult, 8–10 wk old male Sprague-Dawley rats by a single injection of MCT (50 mg kg^{-1} i.p.; Sigma-Aldrich) or an equivalent weight-based volume of sterile saline. Rats weighing >300 g in this age range were utilized for this study due to a decrease in mortality throughout the study. Additionally, this moderate dose of MCT we saw minimal mortality (<2%) and only modest morbidity over the 42-day regimen. For the resveratrol efficacy study, rats were randomly assigned and administered resveratrol (3 mg kg^{-1}; Sigma-Aldrich) or sildenafil (as a clinical reference standard; 175 μg kg^{-1}; AK Scientific) via drinking water beginning at 28 days post MCT injection and continuing for an additional 2 wks. Tap water served as vehicle group for an equivalent duration (28–42 d). Drinking water concentrations of resveratrol and sildenafil were calculated on an observed H_2O consumption of 50 ml/day. As water uptake increases with weight gain, the concentrations were not adjusted and remained constant throughout the course of the study. For time course data, rats (n = 8–12/group) were euthanized at 0, 7, 14, 28, and 42 days post-injection.

2.2 Hemodynamic and Right Ventricular Hypertrophy Measurements

Rats were anesthetized with isoflurane 1–2.5% at 6 mL/min and the right external jugular vein was exposed by blunt dissection. Right ventricular systolic pressure (RVSP) measurements were made via a fluid-filled pressure transducer (Becton Dickinson, DTXplus) were a heparinized (0.01%), saline filled Micro-Renathane catheter (.050 OD × .040 ID) was placed in the right jugular vein. Catheter advancement proceeded until strong positive-negative deflections were observed, indicating catheter placement in the right ventricle, and secured with 4–0 silk suture. Stable RV pressure tracings were collected for 1 min. Blood pressure recordings were obtained at consistent heart rates to minimize variation from isoflurane-induced cardio-depressant effects. Following mid-line thoracotomy, rats were euthanized by exsanguination and the catheter placement in either right ventricle or PA was confirmed. All instrumentation was calibrated prior to experimentation and data (HR, systolic and diastolic RV pressures and $\pm dP/dT$) were collected with a digital acquisition system (Gould Ponemah 7700) connected to a personal computer.

Right ventricular hypertrophy was assessed as the ratio of the right ventricular free wall to the left ventricle plus septum weight (RV/LV+S). Additionally, under light anesthesia, echocardiographic measures of right ventricular performance were obtained one day prior to catheterization using an Acuson Sequoia 512 Ultrasound (Torres et al., 2010). M-Mode measures were used to capture systolic and diastolic dimensions and fractional shortening was calculated as [(end-diastolic - end-systolic) / end-diastolic] × 100 (%).

2.3 Pulmonary Artery Remodeling

Standard histopathology techniques (i.e. hematoxylin/eosin staining) were performed on fixed, paraffin-embedded lung sections (4 μm) to determine a qualitative measure of

vascular remodeling that occurs in the MCT model of PAH. Digital images of pulmonary arteries in three size ranges (< 75 μm, 75–150 μm and > 150μm; n = 8 vessels per size range per subject) were acquired from H/E stained 4 μm sections. Measurements included outer medial and luminal circumference using Image J software (NIH, Bethesda, MD). Vessel diameter was calculated from medial circumference and vessel wall area was calculated by subtracting luminal circumference from outer medial circumference. Furthermore, oblique vessel sections were excluded from analysis.

2.4 Vascular Function Studies

Left and right pulmonary arteries from saline or MCT-injected rats receiving oral (28–42d) resveratrol, sildenafil or tap water were carefully dissected in ice-cold HEPES buffered saline solution (HBSS) containing (in mmol) 150 mM NaCl, 6 mM KCl, 1 mM $MgCl_2$, 1.8 mM $CaCl_2$, 10 mM HEPES, and 10 mM glucose, titrated to pH 7.4 with NaOH and mounted on a wire myograph (DMT). Once mounted, PA rings were bathed in a physiological salt solution (PSS) containing (in mmol) 119 NaCl, 4.7 KCl, 1.17 $MgSO_4$, 1.18 KH_2PO_4, 2.5 $CaCl_2$, 25 $NaHCO_3$, 0.03 EDTA, 5.5 glucose and aerated with a 95% O_2: 5% CO_2 gas mixture at 37°C. Isometric tension was applied (2 mN) and allowed to equilibrate for 30 min prior pre-contraction with 60 mM KPSS solution (equimolar NaCl substitution). Acetylcholine (ACh) concentration response curves were performed after KCl-induced contraction stabilized (20 min) to assess endothelial function and expressed as % reversal of KCl-induced contraction.

2.5 Quantitative Real-Time PCR Analysis

PAs were rapidly dissected from the heart lung bloc in ice-cold saline, snap frozen immediately following RVSP measurement. Total RNA was then isolated from PAs using RNeasy Fibrous Tissue Mini Kit (Qiagen) and quantified by real-time RT-PCR. cDNA was generated using a high capacity reverse transcriptase (ABI) step from 100 ng of RNA using a Peltier thermal cycler (PTC-200, MJ Research). Absolute quantification for dynamic range (serial dilutions of RNA) was performed independently for each primer/dye/probe set to determine amplification efficiency prior to relative PCR analysis. Multiplex real-time PCR amplification of inventoried and custom primer/FAM dye/MGB probe sets (TaqMan, Applied Biosystems) for atrogin-1 (Rn01504258_m1 and Hs01041408_m1), MuRF-1 (Rn00590197_m1), MCIP-1 (Rn00596606_m1), Cbl-b (Rn00709852_m1, $K_v1.5$ (Rn005564245_s1) or eNOS (Rn021326_s1) with respect to β-actin (primer limited VIC or FAM dye/MGB probe-4352340E and 4333762F, respectively) was performed using a 7500 Fast Real-Time PCR System (Applied Biosystems). Relative expression ($^{\Delta\Delta}C_T$) was calculated by subtracting the C_T of the endogenous β-actin control gene from the C_T value of the gene of interest, where the normalized gene expression method ($2^{\Delta\Delta C_T}$) was used for relative quantification of gene expression[1].

2.6 Cell Proliferation, Apoptosis and Sizing

hPASMCs were seeded at 50–60% confluency in a 96-well plate. The following day cells were serum-starved for 24 hrs prior to application of 10 ng/ml PDGF in the presence of vehicle (DMSO: v/v 0.1%), 10, 30, or 100 μM resveratrol for 48 hrs. Proliferation was determined by a fluorescent DNA binding probe (CyQUANT, Invitrogen) by reading at excitation 480 nm/emission 520 nm using a fluorescent microplate reader (Infinite 200 PRO, Tekan). Relative fluorescent light units (RFLUs) were expressed as DNA mass per unit volume (ng/ml) derived from a DNA mass standard curve. The effects of the putative SIRT1 antagonists (25 μM salermide, Sigma; 50 μM sirtinol, Tocris; and 1 μM EX-527, Tocris) were examined in terms of relative atrogin expression as measured by qPCR in quiescent (serum-starved) and proliferating (PDGF-stimulated) hPASMCs. hPASMCs were pre-incubated with these compounds 1 hr prior to PDGF stimulation.

Parallel experiments examined changes in DNA mass (CyQuant) in the presence of these antagonists. Additional experiments examined apoptosis-inducing effects of resveratrol using the early stage apoptosis indicator Annexin V, whereas necrosis (cytotoxicity) was determined by propidium iodide fluorescence. Cells were serum-starved for 24 hours prior to application of PDGF (10 ng/ml) in the presence of vehicle, 10, 30, or 100 μM resveratrol for 48 hrs. The effects of resveratrol on apoptosis and necrosis were determined by measuring Annexin V-FITC (excitation 485 nm/emission 535 nm) and propidium iodide (excitation 560 nm/emission 595 nm) Fluorescence per manufacturers specifications (Cayman Chemical). Quantification of apoptosis and necrosis was performed by a fluorescent microplate reader and expressed as RFLUs. Lastly, the effects of resveratrol hPASMC size was measured with a cell sizer (Z2 Particle Counter & Size Analyzer, Coulter). Cells were serum-starved for 24 hrs, then stimulated with the mitogen PDGF (10 ng/ml) in the presence of resveratrol (vehicle, 10, 30 or 100 μM) for 48 hrs. Trypsinized hPASMCs (~1×10^{-5} cells/T-25 flask) were suspended in a physiological sheath fluid and passed through a 100 μm aperture proximal to a small electrical current. The decrement in the electrical current associated with a single cell passing though the aperture is proportional to cell size. This charge decrement was calibrated to microsphere standards to then determine size in μm. Readings of a 1/1000 dilution (~100–600 cells/run) were made in duplicate and averaged.

2.7 Multiplex Cytokine Expression Assay

Whole blood was obtained via cardiac puncture following RVSP measurements and the resulting plasma was diluted to protein levels (determined by Bradford Assay) as recommended by the manufacturer (Luminex, Austin TX). The Rat Cytokine I 10-plex (Invitrogen) was used to measure a panel of rat cytokines (G-CSF, MCP-1, MIP-1a, IFN-g, GRO-KC, TNF-a, IL-2, IL-4 and IL-6). Assays were performed in a 96-well microplate format according manufactures recommendations, as previously described (Lund et al., 2007).

Statistical Analysis

All data are expressed graphically as means ± S.E. Values of *n* refer to the number of animals in each group. Data were tested for normality and with few exceptions were valid for this assumption (GraphPad Prism v5.02). A one-way or two-ANOVA was used where appropriate for all comparisons between groups. If differences were detected by ANOVA, individual groups were compared with the Student-Newman-Keuls test. Linear trends were conducted in specific sub-set analysis. A probability of ≤ 0.05 was accepted as statistically significant for all comparisons.

3. RESULTS

3.1 Resveratrol Reverses Pulmonary Hypertension and Established Right Ventricular Remodeling

The persistence of elevated hemodynamic variables induced by MCT allowed for an assessment of resveratrol to reverse established PAH. Oral resveratrol and sildenafil (used as a clinical reference standard) treatments initiated 28 days after MCT injection caused a significant reduction in RVSP in MCT-injected rats, with no effect in saline controls (Figure 1A). Right ventricular hypertrophy, measured by RV/LV+S, also declined with resveratrol therapy; however no significant reduction was observed MCT rats receiving sildenafil (Figure 1B). We also observed a slight, yet non-significant decreasing trend in hemodynamic variables between 28–42 day time points (Figure 4A–B). Although cardiac output was not directly measured, RV $+dP/dt$ and fractional shortening were unchanged in MCT rats compared to saline controls, and there was no significant effect of resveratrol or

sildenafil in either group (*data not shown*). Body weights in the study were slightly, but significantly impacted by MCT-treatment, but not by resveratrol (Figure 1C). Similarly, RV thickness, as measured by echocardiography, was elevated in the MCT-treated groups but not reversed by either resveratrol or sildenafil (Figure 1D).

In addition to hemodynamic and right ventricular hypertrophy assessment, we examined the effect of resveratrol in MCT-injected rats on arterial wall thickness of three calibers of pulmonary arteries. MCT caused significant medial hypertrophy in pulmonary arteries across all calibers examined (Figures 2A–C); however MCT rats receiving resveratrol had a partial reduction in wall thickness in vessels ranging from 75 – 150 μm in diameter (Figure 2B). Neither resveratrol nor sildenafil resolved MCT-induced vascular remodeling in vessels less than 75 μm or greater than 150 μm. We also examined markers of systemic inflammation across these groups, but at day 42 there were no apparent elevations in circulating interleukins 2, 4, or 6, TNF-α, IFN-γ, GRO-KC, MIP-1α, MCP-1, or G-CSF caused by MCT (*data not shown*).

3.2 Resveratrol Improves Vascular Function in Established MCT-Induced PAH

Next, we examined whether resveratrol could reverse functional vascular impairments caused by MCT. The net range of ACh-induced relaxation was significantly impaired in preconstricted PAs from MCT-injected rats and resveratrol completely restored vasorelaxation to control levels (Figure 3A). In addition, MCT significantly blunted KCl-induced contraction in PAs, whereas chronic resveratrol treatment enhanced PA contraction (Figure 3B). To ascertain whether the relaxation impairment was a result of the net MCT effects on contraction, we normalized the relaxation values to the magnitude of constriction and still observed a significant impairment of relative relaxation by MCT with complete reversal by resveratrol. Consistent with right ventricular and arterial remodeling, sildenafil had no effect on restoring either ACh-induced relaxations or the diminished contractile phenotype observed in PAs from MCT rats.

3.3 Reductions in Atrogin-1, MuRF-1, eNOS and K_V1.5 are Associated with Experimental Pulmonary Hypertension

We examined the temporal relationship between a number of transcriptional endpoints and the progressive development of MCT-induced PAH. Increases in RVSP in MCT rats were significantly elevated by 14 d and development of right ventricular hypertrophy was evident by 28 d (Figure 4A and B). Interestingly, PA atrogin-1 mRNA expression was significantly reduced from 14 d to 42 d post-MCT injection, which reciprocally paralleled MCT-induced hemodynamic changes. In addition to reductions in atrogin-1 mRNA expression, MuRF-1 expression exhibited a significant declining linear trend to 28 d post-MCT injection; however MuRF-1 expression was significantly elevated at the 42 d time point. In addition to examining atrophic ligase expression, we assessed changes in expression for E3 ubiquitin ligase regulator of phosphotidylinositol-3-kinase (cbl-b; Fang et al., 2001) and found a significant reduction at days 14 and 28 (Figure 4E) suggesting downregulation of E3 ligases that target different growth specific effector molecules such as Akt. Furthermore, account for possible inhibitory influences of the regulatory sub-unit MCIP-1 on CnA (Grammer et al., 2006), we assessed mRNA expression of MCIP-1 but did not observe a temporal relationship between MCT-induce PAH and MCIP-1 expression (Figure 4F). Lastly, we found that eNOS mRNA expression was significantly reduced at 14, and 28 d, but not 42 d post MCT-injection (Figure 4G), while K_V1.5 mRNA expression was reduced from day 14 to 42 d (Figure 4H).

3.4 Resveratrol Restores Atrogin-1 mRNA Expression in Established PAH

Because resveratrol has been linked to activation of FoxO-dependent genes, including atrogin-1 (Ni et al., 2007), we examined the effect of chronic oral resveratrol administration on PA atrogin-1 and MuRF-1 mRNA expression. Chronic resveratrol treatment, but not sildenafil, abrogated the effects of MCT on atrogin-1 expression (Figure 5A). Interestingly, improvements in atrogin-1 expression by resveratrol in MCT rats were tightly associated with decreases in RVSP, RV/LV+S, and PA remodeling (Figures 1 and 2). No effect of resveratrol was seen on MuRF-1 expression (Figure 5B), although there was more sample to sample variability present in this data set. Furthermore, recent reports have demonstrated reductions in eNOS (Csiszar et al., 2009) and $K_v1.5$ channel protein expression (Bonnet et al., 2007) found in MCT-induced PH. Therefore, we assessed whether chronic resveratrol treatment could restore eNOS and $K_v1.5$ expression and found neither of these markers of vascular function were influenced by resveratrol (Figure 5C–D) at 42 d.

3.5 Resveratrol Blunts hPASMC Proliferation and Cell Size

To confirm that resveratrol had direct effects on smooth muscle cell growth and atrogin-1 levels, we conducted a series of *in vitro* studies using human PASMCs. First, anti-proliferative effects of resveratrol were examined in growth-stimulated (PDGF; 10 ng/ml) hPASMCs. PDGF caused a significant increase in hPASMC DNA mass, indicative of a proliferating cell population; however resveratrol (30 and 100 μM) completely abolished the response to PDGF (Figure 6A). Parallel studies examined the relative cytotoxic effects of resveratrol at these concentrations in which no effect was observed (*data not shown*). In addition to anti-proliferative effects of resveratrol, cell diameter was significantly attenuated in growth-stimulated hPASMCs (Figure 6B). The roughly 10% decrease in diameter corresponds to a ~25% reduction in volume based on spherical geometry. Resveratrol did not appear to stimulate apoptosis, rather a mild, yet significant attenuation of programmed cell death was observed at the highest concentration (Figure 6C).

Consistent with *in vivo* findings, resveratrol had a concentration-dependent effect on hPASMC atrogin mRNA expression (Figure 6D). In addition to resveratrol enhancing atrogin expression, atrogin expression was significantly reduced in proliferating hPASMCs compared to serum-starved controls (Figure 6E). Basal atrogin expression was also significantly reduced in serum-starved hPASMCs incubated with the putative SIRT1 selective inhibitors salermide, sirtinol, or EX527 compared to vehicle, but not in proliferating hPASMCs (Figure 6E). The effects of selective SIRT1 inhibition on PDGF-induced increases in DNA mass were also examined. The selective SIRT1 antagonists sirtinol and EX-527 appeared to augment DNA mass in serum-starved hPASMCs, but only EX-527 had this effect in hPASMCs stimulated with PDGF (Figure 6F). These findings suggest that SIRT1 inhibition augments hPASMC proliferation and suppresses atrogin expression.

4. DISCUSSION

In the present study, we documented that resveratrol reversed experimental pulmonary hypertension and further observed that atrophy-related E3 ubiquitin ligase expression was attenuated in pulmonary arteries in the MCT model. To our knowledge this report is the first to document that 1) atrogin-1 and MuRF-1 are expressed in pulmonary vascular tissue and 2) a downregulation of atrophic ubiquitin ligases is associated *in vivo* proliferative pulmonary vascular disease and *in vitro* PASMC proliferation/hypertrophy.

Resveratrol has gained much focus as a potential therapeutic compound for a number of proliferative diseases including neoplastic and cardiovascular disorders. Central to the theme

of resveratrol having anti-inflammatory and anti-proliferative effects in vascular SMCs (Son et al., 2007), a previous study found that chronic resveratrol treatment can prevent increases in MCT-induced RVSP and right ventricular hypertrophy (Yang et al., 2010). Csiszar et al. (2009) also found a similar preventive effect of resveratrol on MCT in terms of hemodynamic indices of PAH and attenuation of inflammatory gene expression, leukocyte infiltration and SMC proliferation. As human PAH is invariably diagnosed well after onset of the pathology, it is important to consider whether potential therapeutics may actually reverse established disease. This study also revealed hemodynamic and molecular variables related to MCT-induced PAH are declining slightly from Day 28 to Day 42, although these trends were never significantly different. It is plausible, given this slight resolution of MCT-induced PAH, a permissive condition for the therapeutic effects of resveratrol during this period may indeed accelerate the reversal of this pathophysiology. Despite this observation, we still see a significant reduction of RVSP and RV/LV+S in the MCT+R group compared to the MCT group. Furthermore, atrogin expression is significantly decreased in the MCT group compared to the Sal group at day and is enhanced in the MCT+R group at the 42 day time-point. We found that chronic oral resveratrol did indeed reverse established MCT-induced PAH and PA dysfunction, although we did encounter a slight reversal of vascular pathology independent of any therapeutic intervention.

Moreover, therapeutic reductions in RVSP and RV/LV+S were achieved with substantially lower oral intake of resveratrol (3 mg/kg/day) compared to those prior studies, suggesting a broader *in vivo* therapeutic range for this compound than previously appreciated. Csiszar and colleagues (2009) used a concentration of 25 mg/kg/day delivered in the drinking water, while Yang et al. (2010) used 20 and 60 mg/kg per day by oral gavage.

We also observed a significant effect of sildenafil, used as a clinical reference standard, to reduce MCT-induced increase in RVSP, although a sparing effect of phosphodiesterase inhibition on right ventricular hypertrophy was not observed. It is unclear why sildenafil, at a modestly higher dose (175 versus 100 μg/kg/day), did not improve RV/LV+S mass over a similar two-week regimen as seen by Schermuly and colleagues (2004). This group used a higher dose of MCT (60 mg/kg), thereby studying the impact of sildenafil on a more severe PAH manifestation. Our regimen did not lead to mortality, unlike the 30–50% mortality observed after 42 days of observation following the 60 mg/kg dose. The higher dose may be more pertinent for human disease, albeit at an accelerated pace, but our goal was to assess effects on a relatively stable, hypertrophied vasculature. A recent study at a much higher dose (10 mg/kg/day) also failed to show a sildenafil effect on RV/LV+S, despite an effect in reducing RVSP (Mouchaers et al., 2010). However, our main finding that resveratrol can therapeutically reverse, not simply prevent, MCT-induced PAH is of potential clinical significance.

In addition to reversing the effects of experimental pulmonary hypertension, there are reports of resveratrol suppressing IL-18-dependent SMC migration (Venkatesan et al., 2009) and angiotension-II mediated aortic SMC hypertrophy (Halder et al., 2002). With respect to SMC proliferation and arterial remodeling within the pulmonary vasculature, Csiszar et al. (2009) clearly demonstrated the preventative effects of resveratrol on arterial remodeling of resistance arteries in MCT rats. Here, we show this effect of resveratrol partially reversing medial wall thickness in intermediate sized (intrapulmonary arteries), but not in resistance or larger conduit arteries. This discrepancy may be due to the moderate concentration and/or route of administration of this poorly bioavailable compound. Another potential explanation for this segmental effect may be that anti-oxidant effects or direct effects on molecular targets of resveratrol (i.e. sirtuin-1) are expressed in a heterogeneous fashion and more susceptible to the actions of resveratrol within this vascular segment. Although others (Yen et al., 2010; Zeng et al., 2010) report reductions in PA remodeling with sildenafil, we did not

observe a reduction in medial wall area possibly due to these prior reports using much higher sildenafil concentrations compared the current study.

Our findings reveal potential parallels between the biochemical pathways that regulate cardiac and skeletal muscle growth and pathological hypertrophy in vascular smooth muscle. The E3 ubiquitin ligases atrogin-1 and MuRF-1 are the molecular determinants that regulate targeted protein degradation of hypertrophic/proliferative proteins such as CnA, MyoD and EIF3 (Lagirand-Cantaloube et al., 2009; Li et al., 2004; Csibi et al., 2009). These ubiquitin ligases couple and post-translationally modify CnA with a lysine 48-linked ubiquitin chain, which targets the NFAT regulating phosphatase for degradation. For example, Li and colleagues (2004) found that atrogin-1 attenuates agonist-induced CnA-dependent activation of NFATc4 and pathological hypertrophy in cardiomyocytes. This report also revealed enhanced CnA signaling and hypertrophy in cardiomyocytes transfected with small interfering RNA for atrogin-1, suggesting that E3 ligases may serve as a key regulatory intersection for NFAT-mediated cell growth. Furthermore, a physiological role for atrogin-1 and MuRF-1 in uterine smooth muscle has been shown (Bdolah et al., 2007), where uterine involution was preceded by a rapid post-partum increase in uterine smooth muscle atrogin-1 and MuRF-1 expression.

More recently, increases in atrogin-1 and Nedd4 expression in biopsies of vastus lateralis muscle in patients with chronic obstructive pulmonary disease where skeletal muscle atrophy is associated with increased mortality (Marquis et al., 2002). Our findings complement the notion that attenuated E3 ubiquitin ligase expression may be relevant markers of PA hypertrophy and these components of the ubiquitin proteasome system may contribute to the pathogenesis of experimental PAH. Although atrogin-1 mRNA expression is reduced in MCT-hypertrophied pulmonary arteries, we were unable to reliably quantify atrogin-1 protein expression with available antibodies, which would have increased our confidence in this conclusion. Given this caveat, further examination of atrogin target protein interactions along with atrogin-1 activity in vascular hypertrophic disease models, both pulmonary and systemic, is warranted. Although cycle threshold for MuRF-1 mRNA was on average 5–6 cycles beyond those of atrogin across all groups suggesting that MuRF-1 is less abundant than atrogin-1, the significant increase of MuRF-1 expression and variability seen at day 42 did not allow for interpretable effects of resveratrol on this E3 ligase. Targeting these proteins may represent a novel therapeutic pathway, although the use of resveratrol is clearly non-specific in modulating atrogin-1 levels and activity.

Therapeutic targeting of the pro-growth Rel family transcription factor NFAT has led to new insights into understanding the pathogenesis of PAH in both human PAH and experimental PAH models (Bonnet et al., 2007). Although we observed a reduction in $K_v1.5$ channel expression, which was hypothesized to be under regulatory control by NFAT, in MCT-pulmonary hypertensive rats, chronic resveratrol treatment did not improve $K_v1.5$ channel expression as a secondary measure of CnA/NFAT activity. Interestingly, a more recent study demonstrated a reduction in KCl-induced contraction that was associated with an increase in pulmonary artery $K_v1.5$ total protein expression in a more acute 22 day MCT pulmonary hypertension model (Dai et al., 2010). Although this report did not determine membrane associated $K_v1.5$ expression, blunted pulmonary artery reactivity to KCl suggests decrease expression or sub-compartment accumulation of the channel which could be explained by increased total protein. Furthermore, improvements in contractile function in MCT rats receiving resveratrol may indicate a role for atrogin-1 that is independent from the CnA/NFAT axis and more related to overall SMC function with regard to other downstream targets of atrogin-1, such as muscle specific differentiating factors or contractile proteins such as MyoD or myosin heavy chain, respectively (Horinouchi et al., 2005; Lagirand-Cantaloube et al., 2009). It is also likely that improvements in atrogin-1 expression in MCT

rats receiving chronic resveratrol are not sufficient to alter $K_v1.5$ expression alone when compared to pharmacological inhibition with CsA (de Frutos et al., 2007; de Frutos et al., 2008) and warrants further approaches that increase atrophic gene product and/or sirtuin-1 expression in hypertrophied SMCs.

In addition to diminished $K_v1.5$ expression as a marker of NFAT activation (Bonnet et al., 2007), we set forth to examine the anti-proliferative as well as atrophic effects of resveratrol in primary hPASMCs. Resveratrol did have a robust anti-proliferative effect and slight, but significant reduction in cell size. The anti-proliferative effects of resveratrol may, in part, be due to inhibition of cell cycle transition between G_0/G_1 to S phase (Poussier et al., 2005), however little is known about the role of E3 ubiquitin ligases such as atrogin on PASMC cell cycle. Along with the profound induction of atrogin mRNA expression by resveratrol, these findings suggest that atrogin expression may influence proliferative and hypertrophic phenotypes in cultured hPASMCs. This finding is supported by our observations that atrogin expression was significantly blunted in PDGF stimulated hPASMCs and appears to be SIRT1-dependent (Figure 6E). It may be likely that downstream PDGF signaling elements, such as PI3K/Akt, may inhibit either FoxO nuclear translocation and/or affinity to the atrogin promoter sequence by phosphorylation of the transcription factor (Essaghir et al., 2009). SIRT1 may have repressive effect on cycle progression, although our data show a link between SIRT1 and atrogin expression it is likely that SIRT1 may indeed regulate other signaling elements governing hPASMC proliferation. Upregulation of atrogin expression in other muscle types, such as skeletal and cardiac myocytes, is a potent inducer of cellular atrophy and contributor to muscle wasting pathologies (Carvalho et al., 2010; Razeghi et al., 2006; Stein and Wade, 2003), rather than an inhibitor of proliferation. Our findings, albeit correlative, support the notion that atrogin expression may indirectly or directly attenuate proliferation, as well as stimulate atrophy in hPASMCs. Contrary to our hypothesis, resveratrol appeared to suppress Annexin V staining in hPASMCs at the maximal concentration employed. This effect was slight, however, and consistent with previous studies where resveratrol protected cardiomyocytes from H_2O_2-mediated apoptosis via a sirtuin-dependent mechanism (Yu et al., 2009). While it has been reported that resveratrol stimulates apoptosis in VSMCs (Poussier et al., 2005), Zou, et al. (1999) documented no such effect.

Although numerous investigations of ubiquitin-mediated proteolytic systems have been conducted in cardiac hypertrophy and skeletal muscle atrophy, a significant gap in knowledge exists with regard to E3 ligase expression in hypertrophied vasculature. Our findings illustrate a temporal reduction in PA atrogin-1 mRNA expression during the development of experimentally induced PAH and a SIRT1-dependent effect on hPASMC atrogin expression and DNA content. Although these conclusions are speculative given the associative trends inherent with the present study design, these data introduce a novel concept of how SIRT1 may modulate the ubiquitin-proteasome system to affect an anti-proliferative phenotype in vascular smooth muscle cells.

Acknowledgments

Funding: This work was funded by a grant from NIH (ES014639).

References

Bdolah Y, Segal A, Tanksale P, Karumanchi SA, Lecker SH. Atrophy-related ubiquitin ligases atrogin-1 and MuRF-1 are associated with uterine smooth muscle involution in the postpartum period. Am. J. Physiol. Regul. Integr. Comp. Physiol. 2007; 292(2):R971–R976. [PubMed: 17008454]

Bonnet S, Rochefort G, Sutendra G, Archer SL, Haromy A, Webster L, Hashimoto K, Bonnet SN, Michelakis ED. The nuclear factor of activated T cells in pulmonary arterial hypertension can be therapeutically targeted. Proc. Natl. Acad. Sci. U.S.A. 2007; 104(27):11418–11423. [PubMed: 17596340]

Budhiraja R, Tuder RM, Hassoun PM. Endothelial dysfunction in pulmonary hypertension. Circulation. 2004; 109(2):159–165. [PubMed: 14734504]

Carvalho RF, Castan EP, Coelho CA, Lopes FS, Almeida FL, Michelin A, de Souza RW, Araujo JP, Cicogna AC, Pai-Silva M. Heart failure increases atrogin-1 and MuRF1 gene expression in skeletal muscle with fiber type-specific atrophy. J Mol Histol. 2010; 41(1):81–87. [PubMed: 20349269]

Chicoine LG, Stewart JA, Lucchesi PA. Is resveratrol the magic bullet for pulmonary hypertension? Hypertension. 2009; 54(3):473–474. [PubMed: 19597034]

Csiszar A, Labinskyy N, Olson S, Pinto JT, Gupte S, Wu JM, Hu F, Ballabh P, Podlutsky A, Losonczy G, de Cabo R, Mathew R, Wolin MS, Ungvari Z. Resveratrol Prevents Monocrotaline-Induced Pulmonary Hypertension in Rats. Hypertension. 2009; 54(3):668–675. [PubMed: 19597040]

Dai ZK, Cheng YJ, Chung HH, Wu JR, Chen IJ, Wu BN. KMUP-1 ameliorates monocrotaline-induced pulmonary artery hypertension the the modulation of Ca2+ sensitization and K+ channel. Life Sciences. 2010; 86(19–20):747–755. [PubMed: 20303989]

de Frutos S, Spangler R, Alo D, Gonzalez-Bosc LV. NFATc3 mediates chronic hypoxia-induced pulmonary arterial remodeling with alpha-actin up-regulation. J Biol Chem. 2007; 282(20):15081–15089. [PubMed: 17403661]

de Frutos S, Duling L, Alo D, Berry T, Jackson-Weaver O, Walker M, Kanagy N, Gonzalez-Bosc L. NFATc3 is required for intermittent hypoxia-induced hypertension. Am J Physiol Heart Circ Physiol. 2008; 294(5):H2382–H2390. [PubMed: 18359899]

Essaghir A, Dif N, Marbehant CY, Coffer PJ, Demoulin JB. The transcription of FOXO genes is stimulated by FOXO3 and repressed by growth factors. J. Biol. Chem. 2009; 284(16):10334–10342. [PubMed: 19244250]

Fang D, Wang HY, Fang N, Altman Y, Elly C, Liu YC. Cbl-b, a RING-type E3 ubiquitin ligase, targets phosphatidylinositol 3-kinase for ubiquitination in T cells. J. Biol. Chem. 2001; 276(7): 4872–4878. [PubMed: 11087752]

Grammer JB, Bleiziffer S, Monticelli F, Lange R, Bauernschmitt R. Calcineurin and matrix protein expression in cardiac hypertrophy: evidence for calcineurin B to control excessive hypertrophic signaling. Basic Res Cardiol. 2006; 101(4):292–300. [PubMed: 16688406]

Haider UG, Sorescu D, Griendling KK, Vollmar AM, Dirsch VM. Resveratrol suppresses angiotensin II-induced Akt/protein kinase B and p70 S6 kinase phosphorylation and subsequent hypertrophy in rat aortic smooth muscle cells. Mol Pharmacol. 2002; 62(4):772–777. [PubMed: 12237323]

Hepple RT, Qin M, Nakamoto H, Goto S. Caloric restriction optimizes the proteasome pathway with aging in rat plantaris muscle: implications for sarcopenia. Am. J. Physiol. Regul. Integr. Comp. Physiol. 2008; 295(4):R1231–R1237. [PubMed: 18703409]

Horinouchi H, Kumamoto T, Kimura N, Ueyama H, Tsuda T. Myosin loss in denervated rat soleus muscle after dexamethasone treatment. Pathobiology. 2005; 72(3):108–116. [PubMed: 15860927]

Humbert M, Morrell NW, Archer SL, Stenmark KR, MacLean MR, Lang IM, Christman BW, Weir EK, Eickelberg O, Voelkel NF, Rabinovitch M. Cellular and molecular pathobiology of pulmonary arterial hypertension. J. Am. Coll. Cardiol. 2004; 43(12 Suppl S):13S–24S. [PubMed: 15194174]

Lagirand-Cantaloube J, Cornille K, Csibi A, Batonnet-Pichon S, Leibovitch MP, Leibovitch SA. Inhibition of atrogin-1/MAFbx mediated MyoD proteolysis prevents skeletal muscle atrophy in vivo. PLoS One. 2009; 4(3):e4973. [PubMed: 19319192]

Li HH, Kedar V, Zhang C, McDonough H, Arya R, Wang DZ, Patterson C. Atrogin-1/muscle atrophy F-box inhibits calcineurin-dependent cardiac hypertrophy by participating in an SCF ubiquitin ligase complex. J. Clin. Invest. 2004; 114(8):1058–1071. [PubMed: 15489953]

Lund AK, Knuckles TL, Obot Akata C, Shohet R, McDonald JD, Gigliotti A, Seagrave JC, Campen MJ. Gasoline exhaust emissions induce vascular remodeling pathways involved in atherosclerosis. Toxicol. Sci. 2007; 95(2):485–494. [PubMed: 17065432]

Marquis K, Debigare R, Lacasse Y, LeBlanc P, Jobin J, Carrier G, Maltais F. Midthigh muscle cross-sectional area is a better predictor of mortality than body mass index in patients with chronic obstructive pulmonary disease. Am. J. Respir. Crit. Care Med. 2002; 166(6):809–813. [PubMed: 12231489]

McFarlane C, Plummer E, Thomas M, Hennebry A, Ashby M, Ling N, Smith H, Sharma M, Kambadur R. Myostatin induces cachexia by activating the ubiquitin proteolytic system through an NF-kappaB-independent, FoxO1-dependent mechanism. J. Cell Physiol. 2006; 209(2):501–514. [PubMed: 16883577]

McLoughlin TJ, Smith SM, DeLong AD, Wang H, Unterman TG, Esser KA. FoxO1 induces apoptosis in skeletal myotubes in a DNA-binding-dependent manner. Am. J. Physiol. Cell Physiol. 2009; 297(3):C548–C555. [PubMed: 19553561]

Mouchaers KT, Schalij I, de Boer MA, Postmus PE, van Hinsbergh VW, Nieuw Amerongen GP, Vonk NA, van der Laarse WJ. Effective reduction of MCT-PAH by Fasudil. Comparison with Bosentan and Sildenafil. Eur. Respir. J. 2010; 36(4):800–807. [PubMed: 20351034]

Murton AJ, Constantin D, Greenhaff PL. The involvement of the ubiquitin proteasome system in human skeletal muscle remodelling and atrophy. Biochim. Biophys. Acta. 2008; 1782(12):730–743. [PubMed: 18992328]

Newby AC, Zaltsman AB. Molecular mechanisms in intimal hyperplasia. J. Pathol. 2000; 190(3):300–309. [PubMed: 10685064]

Ni YG, Berenji K, Wang N, Oh M, Sachan N, Dey A, Cheng J, Lu G, Morris DJ, Castrillon DH, Gerard RD, Rothermel BA, Hill JA. Foxo transcription factors blunt cardiac hypertrophy by inhibiting calcineurin signaling. Circulation. 2006; 114(11):1159–1168. [PubMed: 16952979]

Ni YG, Wang N, Cao DJ, Sachan N, Morris DJ, Gerard RD, Kuro O, Rothermel BA, Hill JA. FoxO transcription factors activate Akt and attenuate insulin signaling in heart by inhibiting protein phosphatases. Proc. Natl. Acad. Sci. U.S.A. 2007; 104(51):20517–20522. [PubMed: 18077353]

Poussier B, Cordova AC, Becquemin JP, Sumpio BE. Resveratrol inhibits vascular smooth muscle cell proliferation and induces apoptosis. J. Vasc. Surg. 2005; 42(6):1190–1197. [PubMed: 16376213]

Razeghi P, Baskin KK, Sharma S, Young ME, Stepkowski S, Essop MF, Taegtmeyer H. Atrophy, hypertrophy, and hypoxemia induce transcriptional regulators of the ubiquitin proteasome system in the rat heart. Biochem. Biophys. Res. Commun. 2006; 342(2):361–364. [PubMed: 16483544]

Schermuly RT, Kreisselmeier KP, Ghofrani HA, Yilmaz H, Butrous G, Ermert L, Ermert M, Weissmann N, Rose F, Guenther A, Walmrath D, Seeger W, Grimminger F. Chronic sildenafil treatment inhibits monocrotaline-induced pulmonary hypertension in rats. Am. J. Respir. Crit. Care Med. 2004; 169(1):39–45. [PubMed: 12958054]

Siddiqui S, Martin JG. Structural aspects of airway remodeling in asthma. Curr. Allergy Asthma Rep. 2008; 8(6):540–547. [PubMed: 18940147]

Son YH, Jeong YT, Lee KA, Choi KH, Kim SM, Rhim BY, Kim K. Roles of MAPK and NF-kappaB in interleukin-6 induction by lipopolysaccharide in vascular smooth muscle cells. J. Cardiovasc. Pharmacol. 2008; 51(1):71–77. [PubMed: 18209571]

Stein TP, Wade CE. Protein turnover in atrophying muscle: from nutritional intervention to microarray expression analysis. Curr. Opin. Clin. Nutr. Metab. Care. 2003; 6(1):95–102. [PubMed: 12496686]

Stenmark KR, Gerasimovskaya E, Nemenoff RA, Das M. Hypoxic activation of adventitial fibroblasts: role in vascular remodeling. Chest. 2002; 122(6 Suppl):326S–334S. [PubMed: 12475810]

Torres SM, Divi RL, Walker DM, McCash CL, Carter MM, Campen MJ, Einem TL, Chu Y, Seilkop SK, Kang H, Poirier MC, Walker VE. In Utero Exposure of Female CD-1 Mice to AZT and/or 3TC: II. Persistence of Functional Alterations in Cardiac Tissue. Cardiovasc. Toxicol. 2010; 10(2): 87–99. [PubMed: 20155331]

Venkatesan BA, Valente J, Reddy VS, Siwik DA, Chandrasekar B. Resveratrol blocks interleukin-18-EMMPRIN cross-regulation and smooth muscle cell migration. Am. J. Physiol. Heart Circ. Physiol. 2009; 297(2):H874–H886. [PubMed: 19561311]

Wilson DW, Segall HJ, Pan LC, Dunston SK. Progressive inflammatory and structural changes in the pulmonary vasculature of monocrotaline-treated rats. Microvasc. Res. 1989; 38(1):57–80. [PubMed: 2503687]

Yang DL, Zhang HG, Xu YL, Gao YH, Yang XJ, Hao XQ, Li XH. Resveratrol inhibits right ventricular hypertrophy induced by monocrotaline in rats. Clin. Exp. Pharmacol. Physiol. 2010; 37(2):150–155. [PubMed: 19566840]

Yen CH, Leu S, Lin YC, Kao YH, Chang LT, Chua S, Fu M, Wu CJ, Sun CK, Yip HK. Sildenafil limits monocrotaline-induced pulmonary hypertension in rats through suppression of pulmonary vascular remodeling. J. Cardiovasc. Pharmacol. 2010; 55(6):574–584. [PubMed: 20224427]

Yu W, Fu YC, Zhou XH, Chen CJ, Wang X, Lin RB, Wang W. Effects of resveratrol on H(2)O(2)-induced apoptosis and expression of SIRTs in H9c2 cells. J. Cell Biochem. 2009; 107(4):741–747. [PubMed: 19415680]

Zeng Z, Li Y, Jiang Z, Wang C, Li B, Jiang W. The extracellular signal-regulated kinase is involved in the effects of sildenafil on pulmonary vascular remodeling. Cardiovasc. Ther. 2010; 28(1):23–29. [PubMed: 20074256]

Zou J, Huang Y, Chen Q, Wang N, Cao K, Hsieh TC, Wu JM. Suppression of mitogenesis and regulation of cell cycle traverse by resveratrol in cultured smooth muscle cells. Int. J. Oncol. 1999; 15(4):647–651. [PubMed: 10493944]

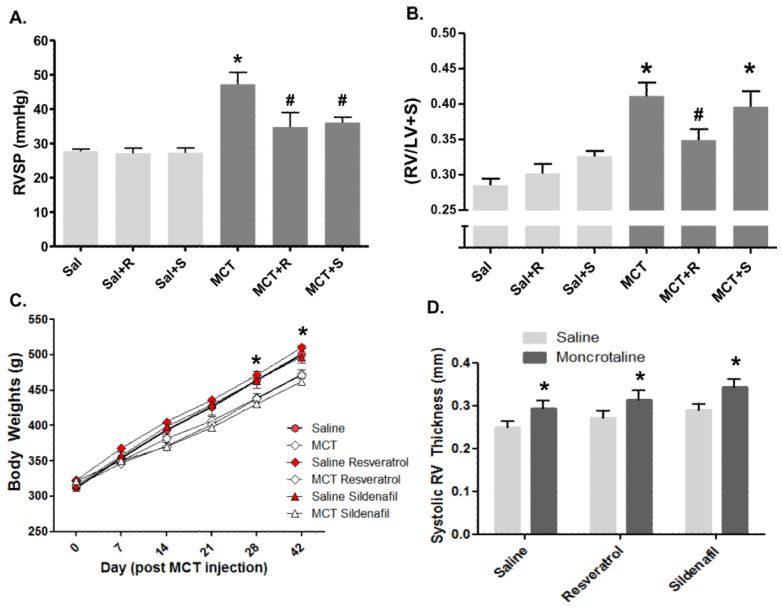

Figure 1.

Resveratrol reverses established pulmonary hypertension and attenuates right ventricular hypertrophy. Rats were injected with saline (Sal) or MCT and followed for 42 days. Resveratrol (R, 3 mg/kg/d) or sildenafil (S, 175 μg/kg/d) was administered via drinking water from 28–42 d post MCT injection. Key indices of pulmonary hypertension, RVSP (A) and RV/LV+S (B) are shown, demonstrating a significant regression in both parameters by resveratrol treatment. Body weights (C) were significantly lower in MCT-treated rats at the end of the study, reflecting a reduction in growth that spanned day 7 to day 21 post-injection. Echocardiographic changes included RV thickening in MCT-treated rats (D), an effect not changed by either resveratrol or sildenafil. Data are expressed as mean RVSP and RV/LV+S ± SEM (n = 8–12 rats). *P < 0.05 versus Sal; #P < 0.05 versus MCT.

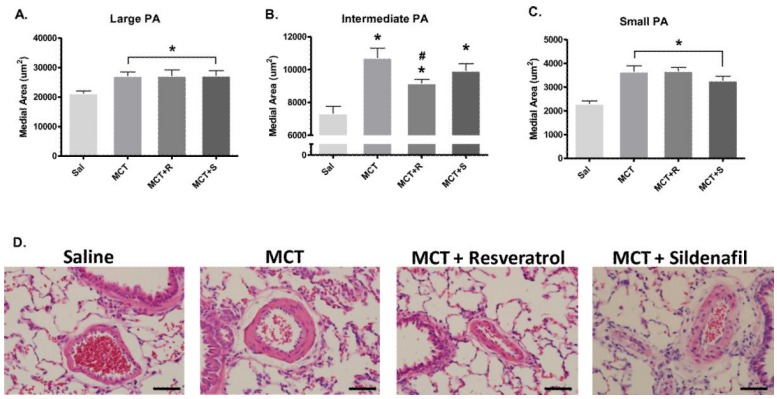

Figure 2.

Resveratrol partially ameliorates MCT-induced pulmonary artery (PA) remodeling in intermediate-sized PAs. Arterial wall thickness was quantified by calculating medial wall area in H/E stained lung sections (4 μm) from A) large (> 150 μm), B) intermediate (75–150 μm) and C) small (< 75 μm) diameter PAs. D) Representative photomicrographs of H/E stained lung sections (from Sal, MCT, MCT+R and MCT+S depicting the effects of resveratrol on PA remodeling. Medial wall area was calculated from 15–16 PAs for each caliber range for each subject. Magnification (objective) 40× and scale bar = 50 μm. Data expressed as mean medial area ± SEM in μm2. *P < 0.05 versus Sal and #P < 0.05 versus MCT.

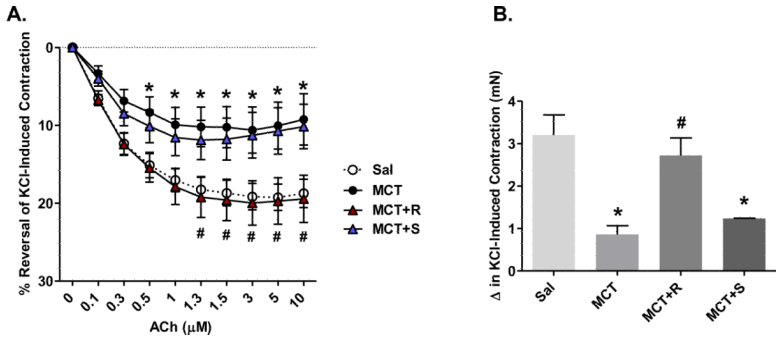

Figure 3.

Resveratrol restores ACh-induced relaxation and KCl-induced contractile responses in PAs from MCT-pulmonary hypertensive rats. Response to increasing ACh concentrations was measured (in mN) by wire myography in PAs pre-contracted with KCl (60 mM). Tension measurements for each group (Sal, MCT, MCT+R and MCT+S) were recorded in response to ACh and expressed as percent reversal of KCl-induced concentration (panel A) or change in KCl-induced contraction (panel B). Data are expressed as mean ± SEM (n = 6–9 rats). *P < 0.05 versus Sal and #P < 0.05 versus MCT.

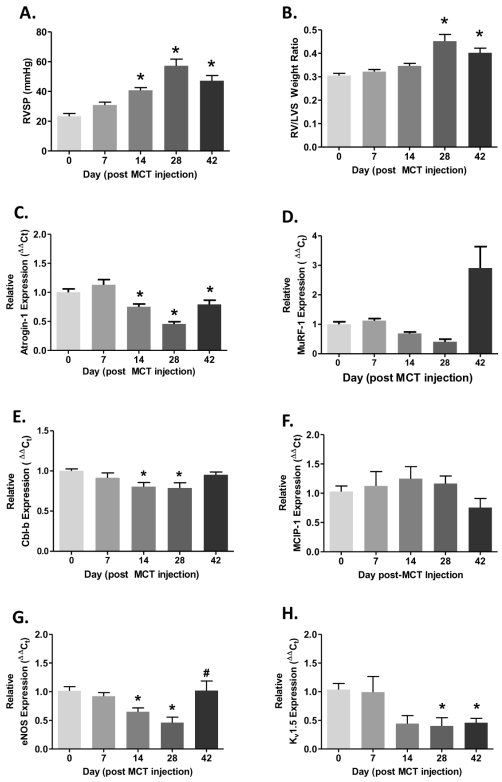

Figure 4.

Development of MCT-induced pulmonary hypertension is associated with transcriptional downregulation of atrogin-1, MuRF-1, eNOS and Kv1.5 mRNA expression. RVSP and RV/LV+S measurements at 0, 7, 14, 28 and 42 days post-MCT injection (A and B). Pulmonary arteries were dissected following RVSP and RV/LV+S measurements and total RNA was extracted for real time PCR analysis for each time point (n = 4–8). Atrogin-1, MuRF-1 and Cbl-b mRNA expression (C, D and E); CnA regulatory subunit MCIP-1 (F); and endothelial NOS and Kv1.5 channel mRNA expression (G and H). RVSP and RV/LV+S data are expressed as mean ± SEM (n = 8 rats) whereas mean target mRNA expression ± SEM is expressed relative to β-actin mRNA expression (ΔΔCt). *P < 0.05 versus baseline (0d); #P < 0.05 indicates significant linear trend from baseline to 28d post-MCT injection.

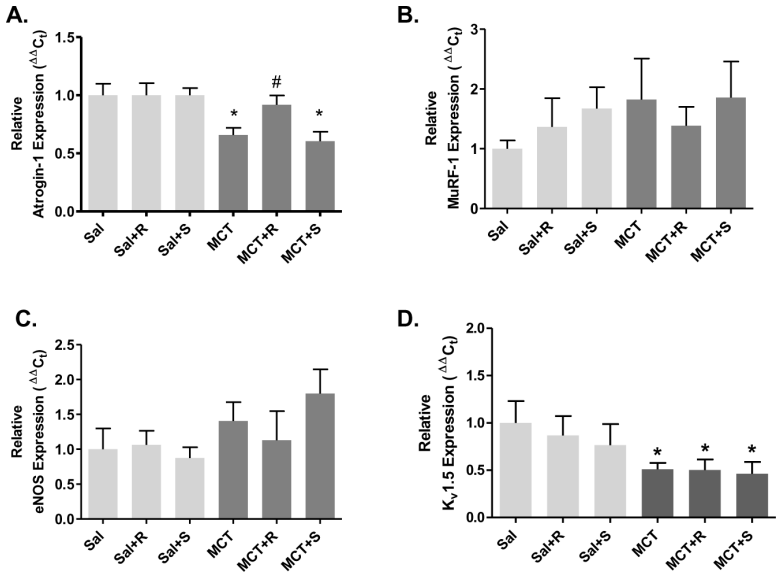

Figure 5.

Resveratrol improves PA atrogin-1 mRNA expression in MCT-induced pulmonary hypertension. PAs were collected for real time PCR analysis after acquisition of hemodynamic indices (figure 1) from Sal or MCT injected rats treated with resveratrol (R, 3 mg/kg/day) or sildenafil (S, 175 μg/kg/day) from 28–42d. Effects of resveratrol on relative mRNA expression for atrogin-1 (A), MuRF-1 (B), eNOS (C) and Kv1.5 (D). Data are expressed as mean target mRNA expression ± SEM is expressed relative to β-actin mRNA expression (ΔΔCt). *P < 0.05 versus Sal; #P < 0.05 versus MCT.

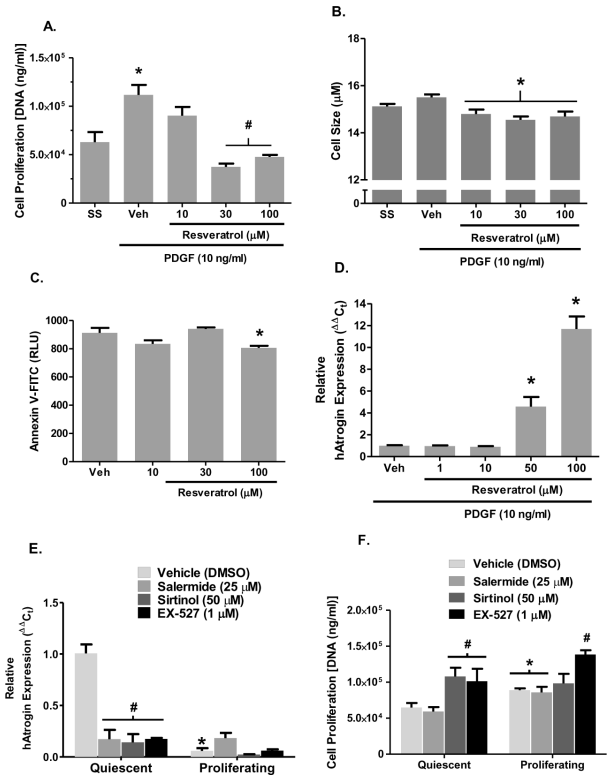

Figure 6.

Summary data illustrating in vitro effects of resveratrol on PDGF-induced proliferation, cell size, apoptosis and atrogin-1 mRNA expression in primary hPASMCs. (A) hPASMC DNA mass was determined by CyQUANT fluorescent assay follow 48 hr exposure to resveratrol in the presence of PDGF (10 ng/ml). (B) Parallel experiments assessed cell size under similar conditions. (C) Annexin V staining was measured in response to increasing concentrations of resveratrol. (D) Quantitative PCR assessing relative atrogin expression in response to 48 hr incubation with resveratrol in the presence of PDGF. Summary data illustrating *in vitro* effects various SIRT1 antagonists on normalized atrogin-1 mRNA expression assessed by qPCR (E) and DNA content in quiescent and proliferating (10 ng/ml PDGF) hPASMCs (F). Data expressed as means ± SEM (n=6/group); symbols * and # indicate $P \leq 0.05$ vs respective control (SS or Veh) by ANOVA.